Left-Handed Double Helical DNA: Variations in the Backbone Conformation

Abstract. *Four different crystals of d(CpGpCpGpCpG) have been solved by x-ray diffraction analysis and all form similar left-handed double helical Z-DNA molecules in the crystal lattice. Two different conformations are observed for the phosphates in the GpC sequences, as the phosphates are found either facing the helical groove or rotated away from it. The latter conformation is often found when hydrated magnesium ions are complexed to a phosphate oxygen atom. These different conformations may be used when right-handed B-DNA joins left-handed Z-DNA. Atomic coordinates and torsion angles are presented for both types of Z-DNA.*

DNA can form both right-handed and left-handed double helical molecules with Watson-Crick base pairing. This is of considerable interest as biological function is often closely correlated with structure on the molecular level. The familiar right-handed helical form of DNA was first described by Watson and Crick in 1953 (*1*). In a fully hydrated medium, DNA is found in what is called the B form (*2*). A number of variations of this basic structure have been described in which there is some alteration in the form of the molecule. The major physical evidence for the structure of DNA comes from x-ray diffraction studies of fibers (*2*). Data from this technique are relatively easy to obtain, but the molecules are disordered to varying degrees and the resolution of the diffraction pattern is correspondingly limited; the data are far from atomic resolution. One can thus rarely solve structures unambiguously from fiber diffraction patterns and they often lead to imprecise structural assignments.

A left-handed double helical form of DNA has recently been described (*3*) in a single crystal of a DNA fragment containing six base pairs with the sequence d(CpGpCpGpCpG) (*4*). The crystal diffracted to 0.9 Å and the structure was solved to atomic resolution, revealing all of the nucleotide components, water molecules, and ions. The ribose-phosphate backbone in this double helix pursues a zigzag course, leading to the name Z-DNA for this left-handed form of the molecule. The crystal contained magnesium and spermine as cations and detailed analysis has revealed that there are two different phosphate conformations present in the polynucleotide backbone. We have now solved three additional, closely related structures which have different cations in their lattices. Comparison of these crystal structures reveals that the conformational alterations in the Z-DNA backbone are common to all four structures. On the basis of these crystallographic analyses, we infer that left-handed double helical Z-DNA molecules can exist as a family of structures with varying conformations of phosphate groups in the sugar phosphate backbone.

Deoxynucleotide tetramers of sequence d(CpGpCpG) form single crystals (*5*) which have recently been solved (*6*, *7*). These also have the same general form of left-handed Z-DNA as reported for the crystalline hexamer fragments, although there are variations in conformation associated with different ions in the lattice.

Crystallographic data on the four closely related crystals of d(CpGpCpGpCpG) are shown in Table 1. As reported earlier, the spermine-magnesium form was solved by the method of multiple isomorphous replacement, using barium, copper, and cobalt derivatives (*3*). The structures of the other complexes were obtained by difference Fourier and constrained refinement methods (*8*) based on the first structure. The full crystallographic details will be published elsewhere. Although the four crystal structures are grossly similar, there were interesting differences between them, some of which will be described here. It should be noted that spermine is not required to form the Z-DNA structure (Table 1).

Structural features of left-handed Z-DNA. Z-DNA forms a helix which contains 12 base pairs per turn of 44.6 Å. In the crystal lattice, the double helical fragments are stacked on each other along the *c* axis as if they were forming a continuous double helix. In fact, the base pairs themselves do form a continuous double helix in the crystal, but the backbone is interrupted every six residues because of the absence of a terminal phosphate group. These molecules form a novel left-handed double helical structure with Watson-Crick base pairs which differs considerably from right-handed B-DNA. The major differences are summarized schematically in Fig. 1. (i) Z-DNA has a sequence of alternating deoxyguanosine and deoxycytidine residues. The asymmetric repeating unit in the structure consists of a dinucleotide, in contrast to the single nucleotide which is the repeating unit in right-handed B-DNA (*2*). (ii) This leaves the double helix with perpendicular pseudodyad axes only between the base pairs but not in the plane of the base pairs. (iii) In Z-DNA, deoxyguanosine is in a *syn* conformation instead of the familiar *anti* conformation of B-DNA (Fig. 2) (*9*). (iv) In addition, its deoxyribose ring has a pucker in which the carbon 3′ is in the *endo* conformation (above the plane of the ring in Fig. 2), in contrast to the C2′ *endo* conformation found in right-handed B-DNA (*10*). (v) Because of this altered conformation of deoxyguanosine, the DNA forms a left-handed double helix in which (vi) the CpG bases are sheared relative to each other, so that the cytosine residues are stacked on each other (Fig. 1). (vii) As a consequence, the guanine residues are no longer stacked on the planar bases, but instead interact with the O1′ atom of an adjacent sugar ring. There are thus two different types of base stacking in the helix depending on the sequence, as GpC differs from CpG in stacking.

Purines are known to form *syn* conformations readily, but *syn* conformations in pyrimidines are less stable for steric reasons (*11*). It is likely that an adenine-thymine pair could adopt a conformation similar to that of the guanine-cytosine pair in Z-DNA (*3*). In forming the left-handed double helix, the base pairs occupy a position at the periphery of the molecule instead of the center, as in right-handed B-DNA. This is shown in Fig. 3, a van der Waals view down the Z-DNA axis of a segment containing three

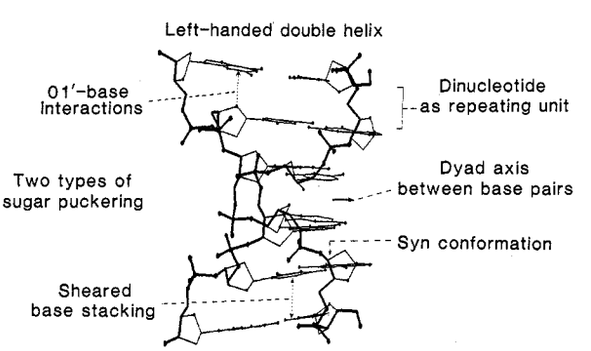

Fig. 1. Schematic diagram showing a projection of the left-handed double helix of the spermine-magnesium d(CpGpCpGpCpG) hexamer. Seven structural features are found in this left-handed DNA conformation which are different from those found in right-handed B-DNA, as indicated in the diagram and discussed in detail in the text.

0036-8075/81/0109-0171$00.50/0 Copyright © 1980 AAAS

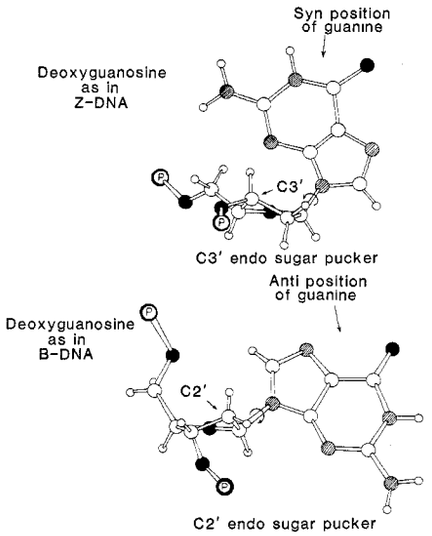

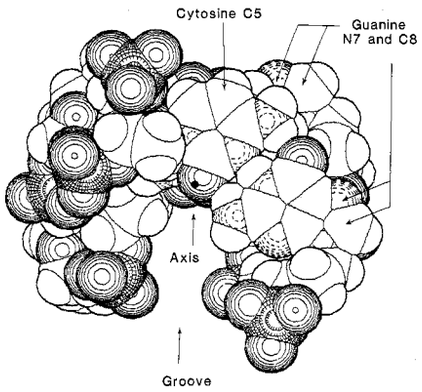

Fig. 2 (left). Conformation of deoxyguanosine in B-DNA and in Z-DNA. The sugar is oriented so that the plane defined by C1′-O1′-C4′ is horizontal. Atoms lying above this plane are in the *endo* conformation. The C3′ is *endo* in Z-DNA while in B-DNA the C2′ is *endo*. These two different ring puckers are associated with significant changes in the distance between the phosphorus atoms. In addition, Z-DNA has guanine in the *syn* position, in contrast to the *anti* position in B-DNA. A curved arrow around the glycosidic carbon-nitrogen linkage indicates the site of rotation. Fig. 3 (right). Van der Waals drawing of a fragment of Z-DNA as viewed down the axis of the helix. Three base pairs are shown, and the deep groove is seen which extends almost to the axis of the molecule. In these three base pairs the groove rotates clockwise toward the reader. For that reason, three phosphates are visible on the left and only one on the right. The N7 and C8 atoms of guanine are near the outer wall of the molecule. This drawing is made directly from the segment of the spermine-magnesium Z-DNA crystal which is in the Z_I conformation. The solid black dot indicates the axis of the molecule.

base pairs. The Watson-Crick G·C base pairs are located at one side of the axis near the periphery of the molecule. Right-handed B-DNA has a major and minor groove, but there is only a single groove in Z-DNA with phosphate groups found along the opening. The single groove in Z-DNA is analogous to the minor groove of B-DNA, while the outer convex surface of Z-DNA is analogous to the concave major groove of B-DNA. As shown in Fig. 3, the outer wall contains segments of the imidazole ring of guanine which are projected outward because of the *syn* conformation of deoxyguanosine.

Two forms of Z-DNA. The pseudo-twofold or -dyad axes between the base pairs relate one chain to another. These dyads are not used in the symmetry of the crystal lattice but are a consequence of interactions within the double helix. The extent to which these are true dyads can be seen in Fig. 4, which shows the conformation of one nucleotide strand (C1 to G6) compared to the other strand (C7 to G12). In forming Fig. 4 the two strands which are antiparallel to each other in the crystal lattice were rotated to show the same view of both. The two strands have a remarkably similar conformation which reflects the internal regularity of the molecule. However, a significant exception is the conformation of the phosphate group lying between G4 and C5 on one strand and G10 and C11 on the other. The conformation of G10pC11 is similar to the conformation of the other two GpC phosphates in the molecule. The phosphate group in G4pC5 has rotated and the phosphorus atom is approximately 1 Å away from the position it occupies in the other three GpC linkages. Further, the C3′-O3′-P-O5′ dihedral angle has rotated about 125°. In the conformation of G4pC5, the phosphate group is in a position where it forms a hydrogen bond to the hydrated magnesium ion which is complexed to the imidazole N7 of guanine 6, as shown in Fig. 4. The magnesium ion has octahedral coordination; one ligand is guanine N7 and the other five are water molecules. Coordination between the phosphate oxygen and the water molecule is quite tight with a phosphate O · · · water O distance of 2.5 Å, indicating a short hydrogen bond. We will designate the majority conformation found in linkages G2pC3, G8pC9, and G10pC11 as Z_I and the conformation found in G4pC5 as Z_{II}. Conformation Z_I is *gauche*(−)-*trans* for the phosphodiester conformation, while Z_{II} is *gauche*(+)-*trans* (*9*). Table 1 shows that the minority conformation Z_{II} appears at C5 in all four of the crystals solved, but it is also partly present in C9 and C11 in two of the crystal forms. In some of the structures, but not in all, G4pC5 is complexed to a magnesium ion as in Fig. 4. In the barium-spermine salt, G4pC5 is in the Z_{II} conformation even though there is no ion coordinated to the guanine of G6. Linkage G8pC9 can also adopt the Z_{II} conformation even though no magnesium ion is present there. In that case two water molecules form a hydrogen bonding bridge from the phosphate oxygen to the imidazole nitrogen of G10 next to it. Thus the phosphate in the Z_{II} conformation may be found coordinated to a hydrated magnesium ion or simply coordinated to water.

The four crystal structures which have been solved have four GpC residues and six CpG residues each, or a total of 16 GpC and 24 CpG linkages. The CpG residues are all in essentially the same conformation, which is probably associated with the shearing of their base stacking mentioned above. However, 5 of the 16 GpC linkages are in the Z_{II} conformation and 11 in the Z_I conformation. This suggests that left-handed Z-DNA molecules may exist in a mixture of conformations ranging from pure Z_I through mixtures of Z_I and Z_{II} to pure Z_{II}. The exact proportions of these two may depend on the

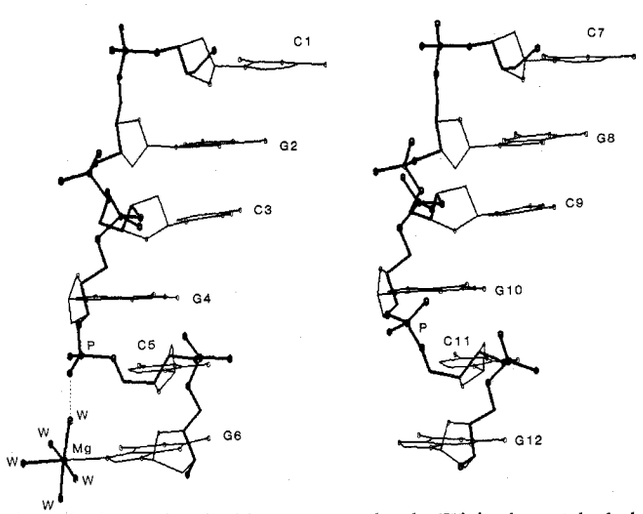

Fig. 4. Diagram showing the conformation of the two independent hexanucleotide molecules in the spermine-magnesium Z-DNA crystal. In the crystal the two strands are antiparallel, but in this diagram they have been arranged in a parallel alignment to show the similarity of the two chains. The two independent chains are very similar except for the linkage G4pC5. That phosphate group has rotated in such a manner that its oxygen is forming a hydrogen bond with a water molecule (*W*) in the octahedral coordination shell surrounding the magnesium ion, which is complexed to N7 of guanine 6.

Table 1. Different crystal forms of d(CpGpCpGpCpG).

Cations in crystal	Mg^{2+}, spermine	Mg^{2+}, spermidine	Ba^{2+}, spermine	Mg^{2+} (and/or Na^{+})
Crystallization conditions*	7 m*M* spermine, 10 m*M* $MgCl_2$	7 m*M* spermidine, 10 m*M* $MgCl_2$	7 m*M* spermine, 10 m*M* $BaCl_2$	10 m*M* $MgCl_2$
Cell dimensions (Å)	a = 17.88, b = 31.55, c = 44.58	a = 17.96, b = 31.19, c = 44.73	a = 17.94, b = 31.54, c = 44.68	a = 17.98, b = 30.94, c = 44.81
Space group	$P2_12_12_1$	$P2_12_12_1$	$P2_12_12_1$	$P2_12_12_1$
Resolution of data used (Å)	0.9	1.3	1.1	1.8
Residual factor	0.13	0.17	0.18	0.13
Residue number in Z_{II} conformation	5	5, 9†	5, 11†	5

*All were crystallized with 20 m*M* sodium cacodylate (*p*H 7.0) and 2 m*M* $d(CG)_3$. †Disordered with both Z_I and Z_{II} conformations.

ionic composition of the medium as well as the local environment of the molecule.

An interesting feature of the two different conformations of the phosphate group in GpC sequences is the altered binding of water molecules. In the Z_I conformation of GpC, the two hydrogen atoms of the guanine N2 amino group both form hydrogen bonds, one to the cytosine O2 to which it is paired and the other to a water molecule. That water molecule in turn forms a hydrogen bond to a phosphate oxygen linked to the deoxyguanosine 3′ hydroxyl group. All of the Z_I conformations of GpC have this bridging water molecule. In the Z_{II} conformation, there is still a hydrogen-bonding bridge, but it involves a chain of two water molecules linking the N2 amino group and the phosphate oxygen. The existence of a single internal bridging water molecule in the Z_I conformation may stabilize it somewhat relative to the conformation of Z_{II}, which has two bridging water molecules. As mentioned previously (*3*), if adenine-thymine base pairs are found in the Z-DNA conformation, they are unable to have the same single bridging water molecule and this may result in some loss of stabilization.

Atomic coordinates of a regular Z-DNA polymer. As noted above, the molecules in these crystals form a virtually infinite double helical polymer of dCpGp, but every third dGpC phosphate group is missing (every sixth phosphate). This polymer has a true 2_1 axis and, if the GpC phosphates are neglected, a very nearly 6_5 axis. The bases of each two consecutive Watson-Crick base pairs are related to each other by a pseudo-twofold axis virtually perpendicular to the 2_1 (or 6_5) axis. Thus we assume that a completely regular polymer will consist of a double helix with a 6_5 helix axis and a

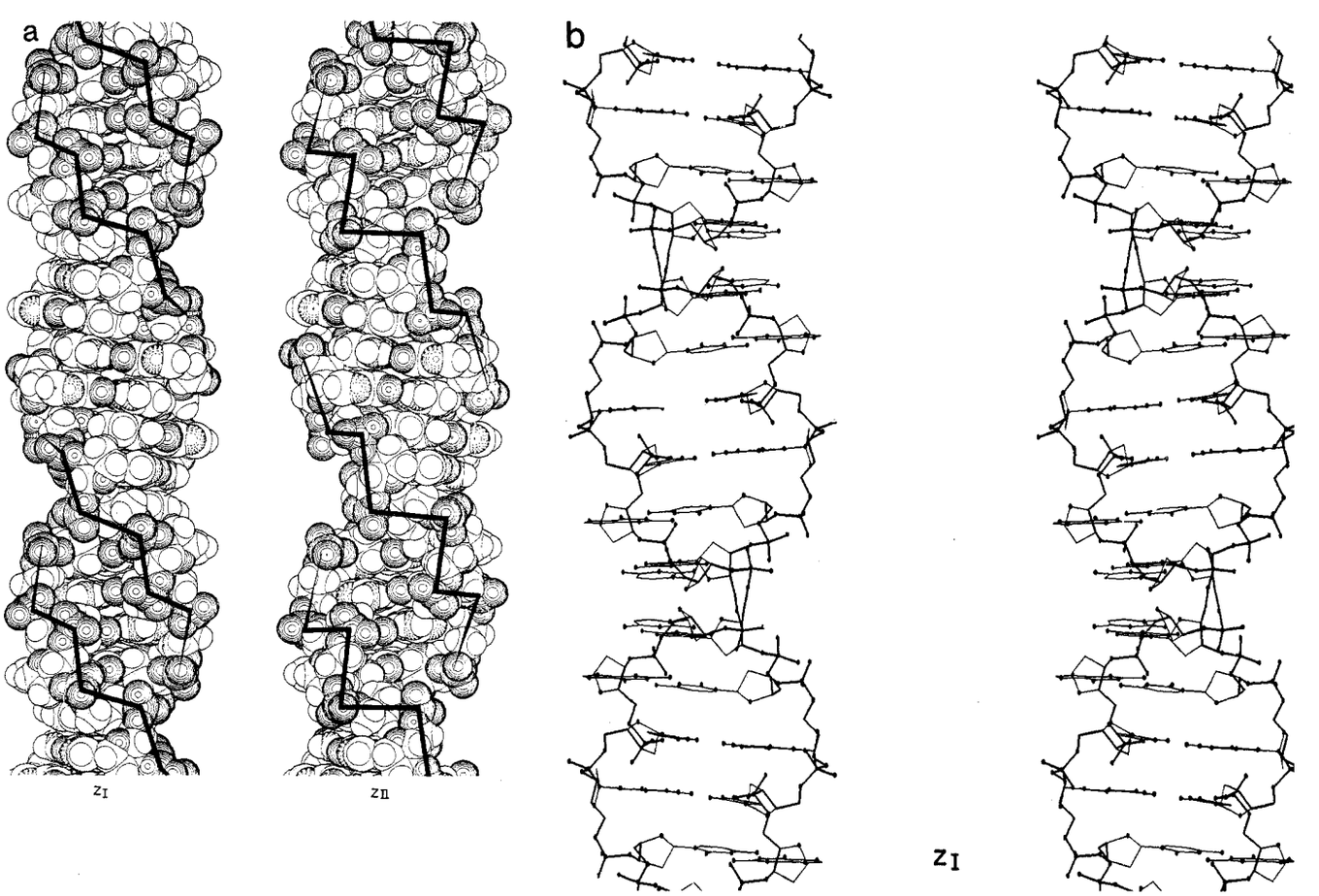

Fig. 5. (a) Van der Waals diagrams of the Z_I and Z_{II} conformations. A solid heavy line is drawn from phosphate to phosphate which shows the zigzag course of the sugar phosphate chain. Because the GpC phosphate group is rotated away from the groove, the zigzag is accentuated in Z_{II} relative to Z_I. (b) Stereodiagram of the regular Z_I helix. This molecule has been generated with the coordinates listed in Table 2.

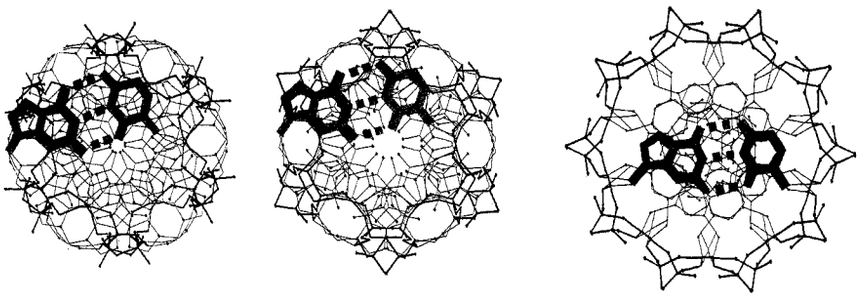

Fig. 6. End views of the regular idealized helical forms of Z_I, Z_{II}, and B-DNA. Heavier lines are used for the phosphate-ribose backbone in a manner similar to that in Fig. 1. A guanine-cytosine base pair is shown by shading. The difference in the positions of the base pairs is quite striking; they are near the center of B-DNA but at the periphery of Z-DNA.

Table 2. Orthonormal and cylindrical coordinates of the Z_I and Z_{II} forms of Z-DNA. Both forms are constrained to have a $6_5 22$ symmetry with a repeat distance of 44.58 Å. The z-axis is the fiber axis and a perpendicular twofold axis is along y at $x = z = 0$. Coordinates for one pCpG sequence including hydrogen atoms are listed. Additional residues and the complementary chain may be generated from these coordinates (*19*).

	Z-I					Z-II				
	X	Y	Z	R	PHI	X	Y	Z	R	PHI
C1P	6.78	2.74	-3.70	7.31	68.8	6.44	4.76	-2.14	8.01	53.5
C101P	6.38	2.01	-4.89	6.69	72.5	5.68	5.67	-1.31	8.02	45.0
C102P	8.17	2.68	-3.22	8.60	71.9	7.90	4.62	-1.92	9.15	59.7
C105'	5.79	2.33	-2.51	6.24	68.1	5.76	3.31	-2.04	6.65	60.1
C1C5'	6.24	1.50	-1.45	6.42	76.5	6.30	2.35	-1.14	6.72	69.6
C1C4'	5.15	0.51	-1.12	5.17	84.4	5.27	1.26	-0.92	5.42	76.6
C101'	3.99	1.23	-0.65	4.17	72.8	4.02	1.85	-0.51	4.42	65.3
C1C1'	2.83	0.79	-1.36	2.93	74.5	2.98	1.42	-1.41	3.30	64.6
C1C2'	3.33	0.25	-2.73	3.34	85.7	3.69	1.04	-2.75	3.84	74.3
C1C3'	4.66	-0.35	-2.32	4.67	94.3	4.94	0.38	-2.16	4.95	85.6
C103'	4.48	-1.78	-1.89	4.79	110.7	4.64	-0.94	-1.75	4.74	101.5
C1N1	1.92	1.96	-1.46	2.74	44.4	2.03	2.55	-1.49	3.26	38.6
C1C2	0.57	1.68	-1.78	1.77	18.7	0.69	2.23	-1.67	2.34	17.1
C1O2	0.17	0.52	-1.82	0.55	18.1	0.31	1.07	-1.76	1.11	16.0
C1N3	-0.38	2.72	-1.60	2.73	353.6	-0.22	3.26	-1.75	3.26	-3.8
C1C4	0.12	3.99	-1.67	3.99	1.8	0.19	4.56	-1.65	4.56	2.3
C1N4	-0.77	4.98	-1.78	5.04	351.3	-0.74	5.51	-1.73	5.56	-7.7
C1C5	1.51	4.28	-1.42	4.54	19.5	1.59	4.88	-1.47	5.13	18.0
C1C6	2.35	3.25	-1.33	4.01	35.9	2.44	3.87	-1.39	4.57	32.2
G2P	5.61	-2.81	-2.03	6.28	116.6	5.67	-2.15	-1.83	6.07	110.8
G201P	5.02	-4.12	-1.84	6.49	129.4	4.98	-3.39	-1.53	6.02	124.2
G202P	6.36	-2.51	-3.27	6.83	111.5	6.39	-2.01	-3.11	6.69	107.5
G205'	6.57	-2.52	-0.78	7.04	111.0	6.70	-1.85	-0.64	6.95	105.5
G2C5'	5.99	-2.33	0.51	6.43	111.2	6.48	-2.41	0.65	6.91	110.4
G2C4'	7.12	-2.11	1.51	7.42	106.5	7.48	-1.71	1.62	7.68	103.0
G201'	7.71	-0.82	1.32	7.76	96.1	7.48	-0.32	1.23	7.49	92.4
G2C1'	7.61	-0.89	2.56	7.81	90.7	7.72	0.45	2.47	7.73	86.5
G2C2'	7.42	-1.87	3.71	7.58	98.2	7.43	-0.44	3.71	7.44	93.4
G2C3'	6.65	-2.14	3.88	6.98	107.9	6.97	-1.74	3.11	7.18	104.0
G203'	6.95	-3.44	3.53	7.76	116.4	7.59	-2.85	3.76	8.10	110.6
G2N9	6.96	1.05	2.46	7.04	81.4	6.87	1.61	2.41	7.06	76.8
G2C8	7.41	2.32	2.41	7.76	72.6	7.33	2.90	2.38	7.88	68.4
G2N7	6.44	3.21	2.30	7.19	63.5	6.37	3.79	2.32	7.41	59.2
G2C5	5.29	2.45	2.28	5.83	65.2	5.22	3.03	2.33	6.03	59.8
G2C4	5.57	1.12	2.37	5.68	79.7	5.48	1.78	2.38	5.74	72.7
G2N3	4.71	0.10	2.38	4.71	88.8	4.62	0.68	2.40	4.67	81.7
G2C2	3.43	0.49	2.29	3.47	81.9	3.35	1.09	2.36	3.52	72.0
G2N2	2.51	-0.41	2.29	2.55	99.4	2.41	0.19	2.37	2.41	85.4
G2N1	3.85	1.79	2.19	3.53	59.6	2.97	2.48	2.31	3.82	51.0
G2C6	3.93	2.85	2.18	4.86	54.1	3.86	3.44	2.29	5.17	48.3
G2O6	3.50	4.02	2.09	5.33	41.0	3.43	4.62	2.24	5.76	36.6
C1HC5'	6.45	2.09	-0.66	6.78	72.1	6.52	2.81	-0.29	7.10	66.7
C1HC5'	7.07	1.03	-1.75	7.15	81.7	7.13	1.97	-1.55	7.40	74.5
C1HC4'	5.53	-0.07	-0.40	5.53	90.8	5.65	0.69	-0.19	5.69	83.0
C1HC1'	2.33	0.08	-0.85	2.33	88.1	2.45	0.64	-1.08	2.53	75.4
C1HC2'	3.46	0.98	-3.40	3.59	74.1	3.92	1.85	-3.30	4.34	64.8
C1HC2'	2.72	-0.45	-3.11	2.76	99.3	3.16	0.40	-3.30	3.18	82.8
C1HC3'	5.30	-0.42	-3.08	5.31	94.5	5.68	0.25	-2.82	5.69	87.5
C1HN4	-0.70	5.90	-1.72	5.94	353.2	-0.71	6.44	-1.69	6.48	-6.3
C1HN4	-1.50	4.81	-1.91	5.03	342.7	-1.47	5.30	-1.83	5.50	-15.5
C1HC5	1.84	5.22	-1.32	5.53	19.4	1.98	5.82	-1.39	6.13	18.1
C1HC6	3.32	3.42	-1.16	4.76	44.1	3.41	4.06	-1.26	5.30	40.0
G2HC5'	5.46	-3.14	0.75	6.30	119.9	6.67	-3.39	0.61	7.48	116.9
G2HC5'	5.39	-1.53	0.47	5.60	105.8	5.52	-2.27	0.98	5.97	112.3
G2HC4'	7.88	-2.81	1.32	8.29	109.8	8.28	-2.17	1.50	8.56	104.7
G2HC1'	8.72	0.38	2.70	8.73	88.8	8.65	0.83	2.47	8.69	84.5
G2HC2'	6.85	-0.63	4.40	6.88	95.2	6.71	-0.05	4.29	6.71	90.5
G2HC2'	8.23	-1.47	4.15	8.36	100.1	8.26	-0.59	4.26	8.28	94.1
G2HC3'	5.67	-2.02	3.15	6.01	109.6	5.99	-1.87	3.27	6.28	107.4
G2HC8	8.38	2.56	2.44	8.76	73.0	8.30	3.13	2.39	8.87	69.3
G2HN1	2.07	1.98	2.13	2.87	46.2	1.99	2.61	2.28	3.28	37.3
G2HN2	2.73	-1.29	2.35	3.03	115.3	2.61	-0.69	2.41	2.78	104.8
G2HN2	1.81	-0.81	2.23	1.81	90.2	1.72	0.61	2.34	1.82	70.3

perpendicular diad relating consecutive base pairs, giving a fiber symmetry of $6_5 22$.

In the crystals, each dCpG (or dGpC) unit is found in a different environment and therefore shows some slight structural variations, as might be expected in an actual polymer. It is thus possible to generate a slightly different idealized polymer based on each of the potential asymmetric units. An idealization procedure was carried out in the following manner: for each dimer the pseudo-twofold axis perpendicular to and through the 2_1 axis was determined only on the basis of the atomic positions of the bases. The twofold related dimer was generated from the 2_1 axis. A helically regular hexamer was then generated with the 6_5 axis and a 44.58-Å repeat, as observed in the crystal. Since the units are not derived from a regular ideal helical polymer, they do not link up perfectly. To correct this, the two hexamers are idealized with a version of the widely used Hendrickson and Konnert (*8*) refinement program modified to maintain $6_5 22$ symmetry in the polymer. To obtain the best model, the target bond distances, angles, and so on were taken as the averaged values from the refined spermine crystal, since these all have the same basic geometry as the polymer. Tables 2 and 3 present coordinates and torsion angles generated for idealized helices in the Z_I and Z_{II} conformations. Side views of the continuous Z_I and Z_{II} molecules are shown in Fig. 5. The zigzag character of the backbone is emphasized in Z_{II} because of the rotation of the phosphate group. Further, the groove is somewhat more open in Z_{II} as the GpC phosphates are rotated away from each other. End views of Z_I and Z_{II} are shown in Fig. 6, together with B-DNA. The Z-DNA molecule has a diameter of 18 Å, compared to 20 Å for B-DNA. The differences in the positions of the base pairs are readily seen.

One of the principal differences between Z-DNA and B-DNA is in the distance between phosphate groups on opposite strands of the molecule. The distance of closest approach in B-DNA is across the minor groove, where phosphate groups are 11.7 Å apart. In marked contrast, the closest phosphate groups are only 7.7 and 8.6 Å apart in Z_I- and Z_{II}-DNA. These are distances between the phosphates of CpG sequences. The closest distances across the chains between phosphates of CpG and GpC sequences are 11.2 and 13.5 Å for Z_I and Z_{II}, respectively. The longer distance for Z_{II} reflects the fact that its GpC phosphates are rotated away from the groove.

These differences between Z_I and Z_{II}

are likely to be important in DNA, which may have adjacent segments of B- and Z-DNA. As mentioned previously, models can be built of joined segments (*3*). The P · · · P separation across the double helix (not the closest distances, however) is 17.4 Å for B-DNA. For Z-DNA, there are two sets of distances, 11.9 Å for the CpG sequences and 14.5 and 16.2 Å for the GpC sequences of Z_I- and Z_{II}-DNA, respectively. The P · · · P separation for CpG is too small to join onto B-DNA; however, the joining can occur at GpC sequences, especially if it is in the Z_{II} form. The P · · · P distances to be joined are within an angstrom of each other: 17.4 Å for B-DNA and 16.2 Å for Z_{II}-DNA. Thus, the suggestion is that the Z_{II} conformation is likely to be found at interfaces of B- and Z-DNA.

Fourier transforms. Using the coordinates in Table 2, we calculated the continuous Fourier transform of Z-DNA (*12*). The major structural component of all the crystals is Z_I and its Fourier transform is shown in Fig. 7. There is a strong meridional reflection on layer line 6, reflecting the dinucleotide repeat, and a very strong meridional reflection on 12, due to the stacking of bases. Strong off-meridional transform components are found on layer lines 2, 8, 13, and 14. The transform of Z_{II} (not shown) has relatively weaker contributions on layer lines 6 and 8 but stronger components on layer lines 1 and 7. Thus the differences in the transforms should make it possible to distinguish the relative proportion of Z_I and Z_{II} in a fiber diffraction pattern.

Arnott *et al.* (*13*) recently presented a fiber diffraction pattern of poly(dG-dC)·poly(dG-dC) which has a *c* axis of 43.5 Å and packs in a hexagonal cell with axes $a = b = 19.1$ Å. Its diffraction pattern agrees quite well with the Fourier transform of Z_I (Fig. 6). The x-ray pattern has strong meridional reflections on layer lines 6 and 12, with the latter much more intense. Furthermore, strong off-meridional reflections are found on layer lines 2, 8, 13, and 14 very close to the peaks shown on the Z_I transform in Fig. 6. The agreement is quite striking, especially in the upper layer lines. However, a quantitative comparison will be necessary in order to determine whether some Z_{II} components are present. The calculations of the continuous Fourier transform were of the unhydrated molecule. In order to make a valid comparison between the observed and calculated diffraction patterns from fibers, it will be necessary to include the ordered water of hydration, which is likely to be firmly bound to the molecule even in the fibrous state. In addition, the packing of the polymer molecules will also affect the agreement between the calculated continuous transform and the observed diffraction pattern.

Table 3. Dihedral angles of DNA (*20*).

	α	β	γ	δ	ϵ	ζ	χ
Z_I-DNA							
C	−137	−139	56	138	− 94	80	21
G	47	179	−169	99	−104	− 69	−112
Z_{II}-DNA							
C	146	164	66	147	−100	74	32
G	92	−167	157	94	−179	55	−118
A-DNA	− 90	−149	47	83	−175	− 45	26
B-DNA	− 41	136	38	139	−133	−157	78

In the hexamer crystals, the base pairs form an infinitely long continuous helix, while the remainder of the molecule forms a continuous helix which is interrupted once every six phosphate groups along the backbone. This suggests that it may also be possible to make a detailed comparison between the diffraction pattern of the crystal and that of the fiber. This will require not only a highly oriented fiber pattern but a detailed study of the manner in which the various hydration sites affect the observed fiber diffraction pattern. Comparison of the crystal pattern and the fiber pattern may thus ultimately lead to considerable insight into the manner in which hydration is maintained in the continuous fiber in comparison to the results observed in the three-dimensional crystal.

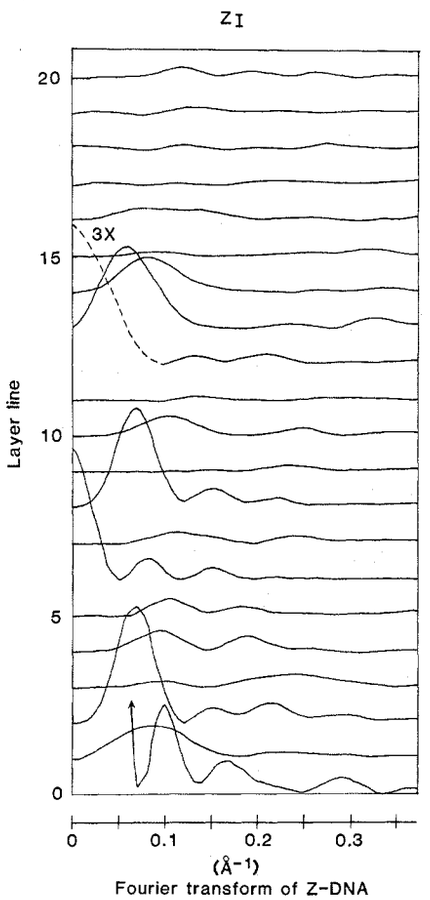

Fig. 7. The continuous Fourier transform of Z_I-DNA. Twenty layer lines are shown and strong meridional reflections are found on layer lines 6 and 12. The former is due to the fact that there are six dinucleotides in the repeating unit; the latter is intense because there are 12 base pairs per turn of the helix oriented almost perpendicular to the fiber axis. Strong off-meridional reflections are seen on layer lines 2, 8, 13, and 14. This transform agrees quite well with the fiber diffraction pattern of poly(dG-dC) (*13*).

Solution studies of poly(dG-dC). Pohl and Jovin (*14*) discovered that poly(dG-dC) could exist in two conformations, depending on the salt concentration. At high salt, the circular dichroism inverted into an unusual form. Patel *et al.* (*15*) carried out a ^{31}P nuclear magnetic resonance (NMR) study of alternating dG-dC oligomers. In high salt, they found two ^{31}P peaks with approximately equal intensity. One of the ^{31}P resonances has a frequency similar to that found in the low-salt form of the polymer, which is the same frequency as that seen for B-DNA. These two peaks reflect the fact that the local environment around the phosphate of dGpC differs in a significant way from that of dCpG. This is a basis for assuming that Z-DNA may be the high-salt form of poly(dG-dC) (*3*). The phosphate in the sequence dGpC can exist in two different forms, which may be associated with coordination of magnesium to N7 of a neighboring guanine residue (Fig. 4). It may thus be possible to identify the two ^{31}P resonance signals, as one of the signals may be responsive to changes in magnesium concentration, leading to the splitting of one of the two peaks because different conformational forms are present.

Different conformations of the polynucleotide backbone have also been observed in other polynucleotides. Wells *et al.* (*16*) stressed the utility of studying synthetic copolymers of alternating sequence. Shifts in the ^{31}P resonance spectra of poly(dA-dT) have been reported which indicate altered conformations of the phosphodiester backbone (*17*). Further, the crystal structure of tetrameric d(pApTpApT) has short double helical stretches in which there are alter-

nating differences in the sugar ring pucker (*18*).

There is considerable utility in presenting idealized coordinates for the two forms of Z-DNA. These can be used for energy calculations to assess the stability of the different conformations; they can also be used in a quantitative analysis of the NMR spectrum as they provide detailed information concerning the environment of various protons in the molecule. The coordinates can also be used to calculate the unique circular dichroism associated with the high-salt form of poly(dG-dC) (*14*). It should be pointed out that these coordinates differ in a significant way from coordinates generated by a study of fiber diffraction patterns. Coordinates from fiber diffraction patterns are generated by making a number of assumptions about the molecule, including the assumption that all repeating units are equivalent; further, conformational details are never visualized in fiber diffraction studies since the analysis is far from atomic resolution. This limitation is important, especially in trying to evaluate NMR spectra, in which small changes in the molecular environment produce considerable changes in the resonance spectrum.

The material presented here suggests that Z-DNA exists not as a single structure but rather as a family of structures which are broadly similar to each other but differ in certain specific ways that result in slightly modified conformations. It is quite likely that changes in local conformation are not confined to Z-DNA alone, but may also be found commonly in the more familiar right-handed B-DNA. Thus local changes in the environment due to ions or proteins are likely to produce changes in conformation, many of which will be sequence-dependent. These changes in conformation may be a significant aspect of the biology of the nucleic acids and may help to define some of the specificity of their interaction with proteins and other molecules.

ANDREW H.-J. WANG
GARY J. QUIGLEY
FRANCIS J. KOLPAK
Department of Biology, Massachusetts Institute of Technology, Cambridge 02139
GIJS VAN DER MAREL
JACQUES H. VAN BOOM
Department of Organic Chemistry, Gorlaeus Laboratories, University of Leiden, Leiden, Netherlands
ALEXANDER RICH
Department of Biology, Massachusetts Institute of Technology

References and Notes

1. J. D. Watson and F. H. C. Crick, *Nature (London)* **171**, 737 (1953).
2. R. Langridge, D. A. Marvin, W. E. Seeds, H. R. Wilson, C. W. Cooper, M. G. F. Wilkins, L. D. Hamilton, *J. Mol. Biol.* **2**, 38 (1960).
3. A. H.-J. Wang, G. J. Quigley, F. J. Kolpak, J. L. Crawford, J. H. van Boom, G. van der Marel, A. Rich, *Nature (London)* **282**, 680 (1979).
4. Abbreviations used in this report: d, deoxy; C, cytosine; p, phosphate; G, guanine; A, adenine, and T, thymine.
5. H. R. Drew, R. E. Dickerson, K. Itakura, *J. Mol. Biol.* **125**, 535 (1978).
6. H. R. Drew, T. Tanako, S. Tanaka, K. Itakura, R. E. Dickerson, *Nature (London)* **286**, 567 (1980).
7. J. L. Crawford, F. J. Kolpak, A. H.-J. Wang, G. J. Quigley, J. H. van Boom, G. van der Marel, A. Rich, *Proc. Natl. Acad. Sci. U.S.A.* **77**, 4106 (1980).
8. W. A. Hendrickson and J. Konnert, *Biomolecular Structure, Conformation, Function and Evolution*, R. Srinivasan, Ed. (Pergamon, Oxford, 1979), vol. 1, pp. 43–57.
9. M. Sundaralingam, *Biopolymer* **7**, 821 (1969).
10. S. Arnott, P. J. C. Smith, R. Chandrasekaran, in *CRC Handbook of Biochemistry and Molecular Biology*, G. D. Fasman, Ed. (CRC, Cleveland, Ohio, ed. 3, 1976), vol. 2.
11. J. M. Neumann, W. Guschlbauer, S. Tran-Dinh, *Eur. J. Biochem.* **100**, 141 (1979).
12. D. R. Davies and A. Rich, *Acta Crystallogr.* **12**, 97 (1959).
13. S. Arnott, R. Chandrasekaran, D. L. Birdsall, A. G. W. Leslie, R. L. Ratliff, *Nature (London)* **283**, 743 (1980).
14. F. M. Pohl and T. M. Jovin, *J. Mol. Biol.* **67**, 375 (1972).
15. D. J. Patel, L. L. Canuel, F. M. Pohl, *Proc. Natl. Acad. Sci. U.S.A.* **76**, 2508 (1979).
16. R. D. Wells *et al.*, *CRC Crit. Rev. Biochem.* **5**, 305 (1977).
17. H. Shindo, R. T. Simpson, J. S. Cohen, *J. Biol. Chem.* **254**, 8125 (1979).
18. M. A. Viswamitra, O. Kennard, P. G. Jones, G. M. Sheldrick, S. Salisbury, L. Falvello, Z. Shakked, *Nature (London)* **273**, 687 (1978).
19. To generate the complementary dimer, use the equation

$$\begin{pmatrix} x' \\ y' \\ z' \end{pmatrix} = \begin{pmatrix} -1 & 0 & 0 \\ 0 & 1 & 0 \\ 0 & 0 & -1 \end{pmatrix} * \begin{pmatrix} x \\ y \\ z \end{pmatrix}$$

To generate the nth neighboring dimer, use

$$\begin{pmatrix} x' \\ y' \\ z' \end{pmatrix} = \begin{pmatrix} \cos[n*(-60°)] & -\sin[n*(-60°)] & 0 \\ \sin[n*(-60°)] & \cos[n*(-60°)] & 0 \\ 0 & 0 & 1 \end{pmatrix} * \begin{pmatrix} x \\ y \\ z \end{pmatrix} + \begin{pmatrix} 0 \\ 0 \\ n*7.43 \end{pmatrix}$$

Where x', y', z' are the new coordinates in angstroms and x, y, z are the original coordinates in angstroms.
20. The dihedral angles are defined as

$$\begin{matrix} & \alpha & \beta & \gamma & \delta & \epsilon & \zeta \\ \text{O3'-P-O5'-C5'-C4'-C3'-O3'-P-O5'} & & & & & & \end{matrix}$$

χ is the angle about the glycosidic bond.
21. This research was supported by grants from the National Institutes of Health, National Science Foundation, National Aeronautics and Space Administration, American Cancer Society, and Netherlands Organization for the Advancement of Pure Research (ZWO).

9 May 1980; revised 27 June 1980

Unmyelinated Axons in the Posterior Funiculi

Abstract. *Electron microscopy of the dorsal funiculus in the rat reveals that most axons in this pathway are unmyelinated. These axons have not previously been counted, nor are they considered in modern studies on the organization of the dorsal funiculus. Because of the importance of this pathway in somatic sensation, it is important to understand that these fibers exist and that they are present in greater numbers than the well-studied myelinated axons.*

The mammalian posterior funiculus is an important somatic sensory pathway in the spinal cord. Textbooks state that the axons in this pathway are predominantly myelinated primary afferent fibers (*1*), and although other fiber types are known, conduction velocities indicate that these others are also myelinated. Furthermore, published histograms of axonal diameters in the posterior funiculus do not mention unmyelinated axons (*2*). Thus it was surprising to find large numbers of unmyelinated axons in each posterior funiculus of the rat. Since the unmyelinated fibers outnumber the myelinated axons in this pathway, it is necessary to ascertain their existence and numbers.

Normal rats were anesthetized with sodium pentobarbital and then perfused through the heart with normal saline. As soon as the right auricular effluent was

Table 1. Number of myelinated and unmyelinated axons in the dorsal funiculus of the S_2 to S_4 segments of the rat spinal cord. The dorsal funiculus proper is that part of the dorsal funiculus that does not include the corticospinal tract.

Rat	Segment	Dorsal funiculus proper		Corticospinal tract		Total	
		Myelinated	Unmyelinated	Myelinated	Unmyelinated	Myelinated	Unmyelinated
1	S_2	5,232	4,609	1,662	2,590	6,894	7,199
2	S_2	5,457	6,452	2,380	2,871	7,837	9,323
3	S_3	3,654	4,338	1,695	2,880	5,299	7,218
4	S_3	3,818	5,214	1,568	2,794	5,386	8,008
5	S_4	2,162	4,702	1,035	3,541	3,197	8,153
6	S_4	3,219	8,186	1,614	3,893	4,833	12,079
Average		3,924	5,584	1,659	3,080	5,574	8,663

0036-8075/81/0109-0176$00.50/0 Copyright © 1980 AAAS